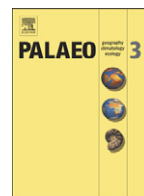




Contents lists available at ScienceDirect

Palaeogeography, Palaeoclimatology, Palaeoecology

journal homepage: www.elsevier.com/locate/palaeo

Antarctic topography at the Eocene–Oligocene boundary

Douglas S. Wilson^{a,*}, Stewart S.R. Jamieson^b, Peter J. Barrett^c, German Leitchenkov^d, Karsten Gohl^e, Robert D. Larter^f^a Marine Sciences Institute, University of California, Santa Barbara, CA 93106, United States^b Department of Geography, Durham University, South Road, Durham, DH1 3LE, UK^c Antarctic Research Centre, Victoria University of Wellington, P.O. Box 600, Wellington, New Zealand,^d Institute for Geology and Mineral Resources of the World Ocean, 1, Angliysky Ave. 190121, St.-Petersburg, Russia^e Alfred Wegener Institute for Polar and Marine Research, Postfach 120161, D-27515 Bremerhaven, Germany^f British Antarctic Survey, Madingley Road, High Cross, Cambridge, Cambridgeshire CB3 0ET, UK

ARTICLE INFO

Article history:

Received 1 November 2010

Received in revised form 12 May 2011

Accepted 16 May 2011

Available online xxxx

Keywords:

Topography

Tectonics

Glacial erosion

Reconstruction

Antarctica

ABSTRACT

We present a reconstruction of the Antarctic topography at the Eocene–Oligocene (ca. 34 Ma) climate transition. This provides a realistic key boundary condition for modeling the first big Antarctic ice sheets at this time instead of using the present day bedrock topography, which has changed significantly from millions of years of tectonism and erosion. We reconstruct topography using a set of tools including ice sheet-erosion models, models of thermal subsidence and plate movement. Erosion estimates are constrained with offshore sediment volumes estimated from seismic stratigraphy. Maximum and minimum topographic reconstructions are presented as indicators of the range of uncertainty. Our results point to a significant upland area in the Ross Sea/Marie Byrd Land and Weddell Sea sectors. In addition, East Antarctic coastal troughs are much shallower than today due to the restoration of material that has been selectively eroded by the evolving ice sheets. Parts of East Antarctica have not changed since the E–O boundary because they were protected under non-erosive cold-based ice. The reconstructions provide a better-defined boundary condition for modeling that seeks to understand interaction between the Antarctic ice sheet and climate, along with more robust estimates of past ice volumes under a range of orbital settings and greenhouse gas concentrations.

© 2011 Elsevier B.V. All rights reserved.

1. Introduction

The aim is to reconstruct the Antarctic landscape at the Eocene–Oligocene (E–O) climate transition (ca. 34 Ma). This is important because experiments to test the sensitivity of ice sheet growth at this time have thus far relied upon the present day subglacial bedrock topography, rebounded for removal of ice load, as a boundary condition (DeConto and Pollard, 2003; DeConto et al., 2007, 2008). These simulations assumed that tectonism and erosion had made no significant changes to the Antarctic landscape over the past 34 million years. However a recent reconstruction of West Antarctica by Wilson and Luyendyk (2009) suggested this region used to lie largely above sea level, with tectonism and erosion shrinking it considerably, reducing the continental area of the whole continent of Antarctica by 10–20% since the Eocene. Land area is a key factor in limiting both present and past continental ice sheet growth and topography determines where ice grows, flows and erodes. Hence the robustness of the results of modeling past ice sheets using different orbital

parameters and greenhouse gas concentrations depends crucially on using a realistic landscape.

This study follows the general method of Wilson and Luyendyk (2009) in separately reversing processes that have changed Antarctic topography: loading of the modern ice sheet; sedimentary deposition, at least for selected continental shelf areas; erosion; thermal subsidence of extended terranes; and horizontal plate motion. We extend the previous work in two important ways: (1) expanding the restoration for erosion to the entire continent, with constraints from estimates of circum-Antarctic sediment volume; and (2) expressing the many significant uncertainties in the reconstruction process by offering separate reconstructions of maximum and minimum topography. We do not claim to present accurate topographic models, but rather two plausible end-members that are more suitable than the modern topography for predicting climate and ice sheet behaviour. We hope that differences in climate or ice sheet predictions between our maximum and minimum reconstructions will inspire further data collection including geophysical mapping and drilling to constrain the gaps in our current knowledge. Because of the limited resolution that is currently feasible for long-term climate and ice models, we generally do not address features smaller than about 40 km. We do not systematically address the evolution of deep-water bathymetry (below ~1000 m). That issue will be addressed by the ongoing work of

* Corresponding author. Tel.: +1 805 893 8033; fax: +1 805 293 2314.

E-mail addresses: dwilson@geol.ucsb.edu (D.S. Wilson),Stewart.Jamieson@dur.ac.uk (S.S.R. Jamieson).

the Circum-Antarctic Stratigraphy and Paleobathymetry (CASP) project of a working group under the Scientific Committee for Antarctic Research (SCAR) Antarctic Climate Evolution program.

The techniques employed in our reconstruction are simple, with detailed explanations only for our method for flexural isostatic compensation with partial flooding of the continent, and our model for glacial erosion of the East Antarctic craton (Section 3 below).

2. Geologic background

2.1. Regional tectonics

The Antarctic continent is generally recognized as having a long-stable, East Antarctic sector (Fig. 1), with little Mesozoic or Cenozoic tectonic activity other than passive-margin formation with the rifting of Gondwana (e.g., Lawver and Gahagan, 1994). The West Antarctic sector has been more active with considerable Cretaceous and Cenozoic activity including subduction, gradually decreasing from most of the margin in the Early Cretaceous to hardly any in the late Cenozoic (e.g., Larter et al., 2002), extensional rifting in the West Antarctic Rift System (Behrendt et al., 1991), and volcanism. The Transantarctic Mountains, a major range with many peaks above 4000 m, form the boundary between East and West Antarctica. Several lines of evidence indicate that the modern relief in these mountains was largely established ~55–35 Ma, with subsequent glacial erosion strongly affecting only limited areas (e.g., Sugden and Denton, 2004; Miller et al., 2010).

The history of tectonic extension in the WARS is only broadly understood, as most of the extended area is hidden beneath the Ross Ice Shelf. Extension in western Marie Byrd Land and the eastern Ross Sea has been dated at 90–100 Ma (Fitzgerald and Baldwin, 1997; Luyendyk et al., 2003; Siddoway et al., 2004). The youngest phase of extension is better understood, having been interpreted from the seafloor spreading record of motion between East Antarctica and West Antarctica in the northwestern Ross Sea (Cande et al., 2000).

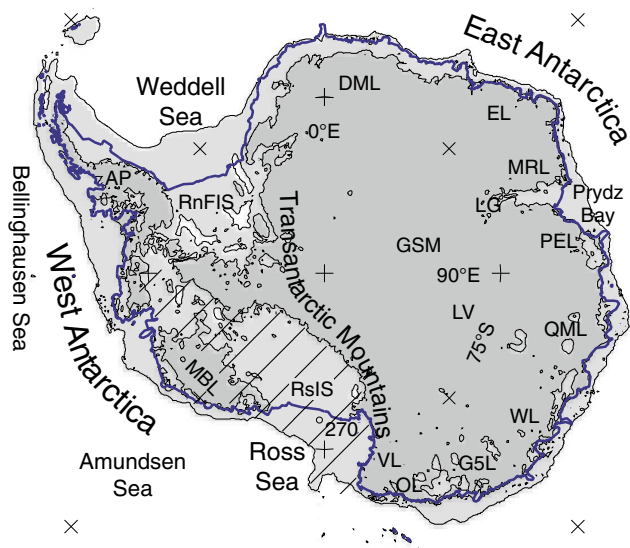


Fig. 1. Location map. Bold line shows recent Antarctic coastline, including ice shelves. Darker gray shading shows bed elevation above modern sea level, after applying a rebound correction for ice load (Fig. 2b); lighter shading shows bed shallower than –1000 m. Hachures show West Antarctic Rift System, active in Late Cretaceous and Cenozoic (Behrendt et al., 1991). Abbreviations: DML, Dronning Maud Land; EL, Enderby Land; MRL, MacRoberston Land; PEL, Princess Elizabeth Land; QML, Queen Maud Land; WL, Wilkes Land; GSL, George V Land; OL, Oates Land; VL, Victoria Land; MBL, Marie Byrd Land; AP, Antarctic Peninsula; LG, Lambert graben; GSM, Gamburtsev Subglacial Mountains; RnSIS, Ross Ice Shelf; RnFIS, Ronne-Filchner Ice Shelf; 270, DSDP Site 270.

Spreading there since 45 Ma is ~170 km, and since 34 Ma is ~70 km. Total extension of the WARS can only be inferred from indirect arguments; estimates range about 300–600 km (Behrendt et al., 1991; Cande et al., 2000; Wilson and Luyendyk, 2009).

2.2. Sediment volume

The strongest constraint on the extent of continental erosion is the volume of sediment deposited around the continent. For Oligocene and younger, sediment distributions are fairly well mapped in the shallow Ross Sea, most of the East Antarctic margin, and the eastern Weddell Sea. In contrast, the western Weddell Sea and areas under the Ross, Ronne, and Filchner Ice Shelves are almost totally unmapped. For the purpose of estimating minimum and maximum palaeo-topographic surfaces, we separately estimate minimum and maximum sediment volumes, as well as densities and the biogenic fraction needed to calculate the original volume of the source material.

For the Indian Ocean sector, our observed volumes are based on the work of Kuvaas et al. (2004) and Leitchenkov et al. (2007, 2008) (Table 1). The sediment is almost entirely in deep water. We estimate volume uncertainty at $\pm 10\%$ except for the eastern subdivision which increases to $\pm 20\%$ due to limited mapping.

In the Ross Sea, our estimates are based on the volume of sedimentary units RSS-2 and younger from ANTOSTRAT (1995). Units are well mapped on the continental shelf, poorly mapped in deep water, and unmapped under the Ross Ice Shelf. Significant uncertainty also arises because there is only a minimum age for the base of RSS-2 at ~26 Ma (McDougall, 1977; ANTOSTRAT, 1995); we account for the possibility that a significant volume of sediment below RSS-2 is younger than 34 Ma. In parts of the Ross Sea, considerable thicknesses of sediments judged to be older than 34 Ma are not restored.

For the Amundsen Sea and western Bellinghousen Sea sector, our estimates are derived from the isopach grids of Scheuer et al. (2006a) and additional thickness estimates from more recently acquired seismic data in the southern Amundsen Sea (K. Gohl, unpublished). The seismic horizons which are interpreted as the onset of glacially deposited sediments (e.g., Nitsche et al., 2000) are correlated from the drilled and dated continental rise records of the Antarctic Peninsula, through the Bellingshausen Sea (Scheuer et al., 2006b), and farther to the Amundsen Sea. With no drill records in this latter sector, any age estimate for the major onset of deposition of glacially transported sediments on the shelf and continental rise remains speculative. Whilst glacially-derived sediments were accumulating on the Antarctic Peninsula continental rise since at least 9.5 Ma, the timing of onset of glacial sedimentation in the southern Bellinghousen and Amundsen seas is presently unconstrained by drilling and may have occurred either earlier or later than along the Antarctic Peninsula. Uncertainties are large due to incomplete mapping and limited age control.

Sediment volumes along the Antarctic Peninsula are based on seismic data from Tucholke and Houtz (1976), Larter and Barker (1991), Nitsche et al. (1997, 2000), and Cooper et al. (2009), with age control from DSDP Sites 322 and 325 (Hollister and Craddock, 1976). We set a significant upper bound for volume based on the possibility of substantial sediment subduction beneath the northern Peninsula.

Sediment volume for the Weddell Sea is primarily derived and extrapolated from the seismic stratigraphy mapped by Rogenhagen et al. (2004) in the eastern Weddell Sea, with age control from ODP Site 693 (Barker et al., 1988; Miller et al., 1990). Extrapolation was guided by the very few existing seismic records (Hübscher et al., 1996; Rogenhagen and Jokat, 2000). Uncertainty is large and can only be estimated subjectively, due to lack of data under nearly permanent sea ice. We assume the transition between net deposition and net erosion since 34 Ma occurs north of the Ronne-Filchner Ice Shelf.

Table 1
Observed sediment volume and source estimates.

Region		Observed Volume 10 ⁶ km ³		In situ density (g/cm ³)		Biogenic fraction		Source density (g/cm ³)		Target source volume 10 ⁶ km ³	
Name	Longitude	A–Min	B–Max	A	B	A	B	A	B	A–Min	B–Max
DML	0°–30°E	0.54	0.66	1.95	2.15	0.15	0.05	2.6	2.5	0.34	0.54
EL	30°–60°E	0.63	0.77	1.95	2.15	0.15	0.05	2.6	2.5	0.40	0.63
MRL-PEL	60°–94°E	1.17	1.43	1.95	2.15	0.15	0.05	2.6	2.5	0.75	1.17
QML-WL	94°–124°E	0.54	0.66	1.95	2.15	0.15	0.05	2.6	2.5	0.34	0.54
G5L-OL	124°–165°E	0.48	0.72	1.95	2.15	0.15	0.05	2.6	2.5	0.31	0.59
Ross	165°E–150°W	1.50	3.00	2.10	2.30	0.15	0.05	2.6	2.4	1.03	2.73
Bell-Amun	150°–80°W	1.60	2.60	1.95	2.15	0.15	0.05	2.6	2.4	1.02	2.21
W Penins	80°–50°W	1.00	2.00	1.95	2.15	0.15	0.05	2.6	2.4	0.64	1.70
Weddell	~50°W–0°	2.40	4.40	2.10	2.30	0.15	0.05	2.5	2.3	1.71	4.18
Totals		9.86	16.24							6.54	14.29

Target volume = Obs Vol. × (1.0 – BioFrac.) × IDens/SDens. Region abbreviations from Fig. 1.

The factors relevant for converting sediment volume to source volume are not well known. We assume a biogenic fraction, which we do not restore to the continent, of 5–15%, guided by DSDP and ODP results around Antarctica. We assume a minimum in-situ density of 1950 kg/m³ for thinner, deep-water sediments and a maximum of 2300 kg/m³ for thicker, shelf sediments. Density of the original source is assumed in the range of 2500–2600 kg/m³ for the East Antarctic craton, but possibly as low as 2300 kg/m³ for a largely sedimentary source for the Weddell Sea. There is a clear division of Nd-isotope populations of young sediments into East- and West Antarctic sources (Roy et al., 2007), suggesting that the sediments are largely derived from the adjacent part of the continent.

2.3. Climate history

To understand the glacial regime under which the Antarctic landscape evolved, the stepwise glacial history of Antarctica is pieced together (Table 2). As will become clear, our approach relies on modeling glacial extents in East Antarctica. Following the growth of an initial continental-scale ice sheet at 34 Ma (Barrett, 1989; Hambrey et al., 1991; Zachos et al., 1992; Zachos and Kump, 2005) ice sheets did not permanently stabilise at the coast. Isotopic records show that the initial ice sheet had reduced in size by 33.6 Ma (Zachos and Kump, 2005) and the preservation of *Nothofagus* pollen assemblages in the CIROS-1 and CRP-3 cores suggest that the climate was at times similar to present day southern Patagonia (Mildenhall, 1989; Raine and Askin, 2001). After 33.6 Ma the ice sheet margin oscillated in pace with orbital cycles until at least 17 Ma as recorded by sedimentary

cycles in the Cape Roberts cores (Cape Roberts Science Team, 1999, 2000; Fielding et al., 2000; Naish et al., 2001; Barrett, 2007) and isotopic records suggest this cyclicity probably continued until the mid-Miocene (Pekar and DeConto, 2006). Ice sheet modeling forced by orbital cycles under a reduced atmospheric CO₂ indicate these fluctuations may have been on a similar scale to those of northern hemisphere Pleistocene ice sheets (DeConto and Pollard, 2003; Jamieson and Sugden, 2008) and probably represented Antarctic ice volumes ranging between ca. 10 and ca. 21 million km³, or 24 to 50 m of sea level equivalent (Bertler and Barrett, 2010).

A 6–7 °C reduction in Pacific surface water temperature records mid-Miocene cooling at around 14.2–12.7 Ma (Shevenell et al., 2004; Holbourn et al., 2005) and was experienced onshore as a transition from warm- to cold-based localised glaciation in the Transantarctic mountains (Lewis et al., 2007) and by an expansion of continental ice under a hyperarid polar climate. By ca. 14 Ma the ice sheet achieved its maximum extent, reaching the continental shelf edge in most areas (Sugden and Denton, 2004). However, by 13.6 Ma the ice sheet had retreated and in East Antarctica had dimensions similar to present day, fluctuating in response to sea level and ocean temperature changes for the majority of the period until present and occasionally expanding to the continental shelf edge (Denton and Hughes, 1986; Anderson, 1999; Sugden and Denton, 2004; Mackintosh et al., 2007; Cooper et al., 2009; Mackintosh et al., 2011).

The glacial history of West Antarctica is more dynamic and less certain. Stratigraphic evidence from the Ross Sea has been used to suggest that during the Pliocene it advanced onto the continental shelf in the Ross Sea multiple times (Bart, 2001) and collapsed

Table 2
Stepwise climate variability.

Time (Ma)	Ice configuration	Evidence
34.0–33.6	Continental ice sheet initiation.	Initial continental-scale ice recorded in oxygen isotope and sedimentary records (Barrett, 1989; Hambrey et al., 1991; Zachos et al., 1992; Zachos and Kump, 2005).
33.6–14.0	Fluctuations between near modern and near fully deglaciated states.	Ice reduced in scale by 33.4 Ma (Zachos and Kump, 2005) and <i>Nothofagus</i> pollen in CIROS-1 and CRP-3 indicates conditions similar to present-day Patagonia (Mildenhall, 1989; Raine and Askin, 2001). Sedimentary cycles in Cape Roberts (Cape Roberts Science Team, 1999; 2000; Barrett, 2007; Fielding et al. (2000); Naish et al. (2001). Model comparison with geomorphology suggests ice volume range of 10–25 million km ³ (DeConto and Pollard, 2003; Jamieson et al., 2010).
14.0–13.6	Maximum polar ice sheet.	Step cooling in ocean waters (Shevenell et al., 2004; Holbourn et al., 2005). Switch from warm- to cold-based glaciers in Victoria Land (Lewis et al., 2007). East Antarctic ice sheet stabilises. Ice reaches continental shelf edge (Anderson, 1999).
13.6–0.0	Similar to present day and fluctuating in response to sea level.	Ice retreats from shelf edge by ca. 13.6 Ma (Anderson, 1999; Sugden and Denton, 2004). Hyper-arid polar conditions prevail (Denton et al., 1993). West Antarctic ice sheet collapses and reforms in the warmer climate that prevailed until 3–2 Ma ((Naish et al., 2009; Pollard and DeConto, 2009) after which both ice sheets fluctuate in a reduced way in response to sea level changes from growth and collapse of N Hemisphere ice sheets (Denton and Hughes, 1986; Mackintosh et al., 2007).

periodically (Naish et al., 2009). Modeling suggests collapse (up to +7 m sea level equivalent) could be driven by obliquity-paced ocean-induced melting under globally higher temperature and CO₂ conditions (ca. 3 °C above present and 400 p.p.m.v.; Pollard and DeConto, 2009). Collapses may not have been limited to the Pliocene and the presence of late Pleistocene diatoms beneath the Whillans ice stream suggests that there was a more recent collapse of the West Antarctic Ice Sheet (Scherer et al., 1998). Conversely, the lack of erosional features on volcanoes in Marie Byrd Land has led to suggestions that a stable cold climate has existed since the mid-Miocene (Rocchi et al., 2006).

3. Modeled processes

Our approach is to integrate simulations of ice sheet behaviour, glacial erosion, tectonics, plate movement and lithospheric dynamics to reconstruct the palaeotopography of Antarctica at the E–O transition. The reconstruction is constrained using local-, regional- and continental-scale evidence for the pattern of landscape evolution as well as an understanding of landscape evolution gained from the beds of former northern hemisphere ice sheets.

3.1. Flexural isostasy

Many steps of our reconstructions incorporate flexural isostatic response to changes in surface loads. We use the standard model of a thin elastic plate overlying an inviscid fluid, implemented using Fourier transforms following Banks et al. (1977). The effective elastic thickness of the plate is a free parameter of the model; for simplicity we use a uniform value of 35 km for the entire continent, which is neither absurdly low for the East Antarctic craton nor absurdly high for recently active West Antarctica. It is common for the flexure model to predict partial flooding or emergence of continental areas. This flooding or emergence changes the load imposed by water on the top of the plate, indicating that a simple, single-step calculation does not accurately reflect the flexural response. We therefore iterate toward an internally consistent model by using the flexed topography to calculate a new water load, and repeat the process several times until the magnitude of flexure is less than a few meters. The reconstructed pre-glacial water load also includes the effect of adding the modern Antarctic ice to the ocean, which we approximate as a simple 60-m sea level rise, ignoring spherical-earth effects.

3.2. Glacial erosion model

Erosion of sediment by ice is the most widely distributed physical process that we aim to account for in this reconstruction. We use the GLIMMER-CISM 3-dimensional ice sheet model (Rutt et al., 2009) with a coupled erosion model (Jamieson et al., 2008) to understand patterns of long-term glacial landscape evolution. The ice sheet model uses the shallow ice approximation and therefore assumes that ice surface and bed slopes are shallow and thus that longitudinal stress has a negligible effect upon ice behaviour (Hutter, 1983). Given that we model ice configurations at a 20 km resolution this assumption is robust. The model is thermomechanically coupled and therefore enables the pattern of basal melting and basal ice velocity to be simulated.

Glacial erosion occurs where there is water at the base of the ice to provide lubrication between the ice and its bed to enable sliding (Boulton, 1972). Therefore, modeled erosion patterns are determined by the distribution of basal melt-rates (as a proxy for water pressure) at the ice sheet base, basal sliding velocity and lithological susceptibility to erosion. The latter term is treated initially as a constant due to the inaccessibility of the Antarctic bed as is geothermal heat flux which is important for predicting melting (Näslund et al., 2005; Jamieson et al., 2008), but for which no long-

term reconstruction exists. Basal sliding velocity is controlled by basal shear stress and a 'slipperiness' parameter describing the tractive conditions at the ice/bed interface. This 'slipperiness' term is modeled as a function of basal melt-rate such that as pressure melting point is reached and melting begins and increases, the most rapid increase in slip (and therefore basal sliding velocity and erosion) is felt at low melt-rates (Jamieson et al., 2008). By tuning the relationship between basal melt-rate and slip it is possible to alter the sensitivity of glacial erosion to basal velocity. This can ensure that constrained incision depths (e.g. the depth of a coastal trough) are achieved whilst also balancing a basin-wide sediment budget against offshore volume constraints. Where there is no basal melting in the model, the ice sheet is frozen to its bed and therefore protects the landscape from erosion. Such a model is well suited to understanding landscape evolution in regions like East Antarctica where the ice sheet is terrestrial and topographically confined (Jamieson and Sugden, 2008; Jamieson et al., 2010).

4. Reconstruction steps

We describe our reconstruction steps in the order they are performed. The amplitude of the isostatic response to each step can depend on the sequence because of the sensitivity of water load to the intermediate steps. We perform the erosion restoration after horizontal plate motion, as this sequence simplifies generating sensible models in the area of faults modeled as active in the Oligocene but not since, with abrupt changes across the speculatively-located faults present in the thickness of the erosion restoration but not the modern topography. Revisions from the Wilson and Luyendyk (2009) model are extensive for restoring erosion. However, for other processes we follow the Wilson and Luyendyk (2009) approach closely, but incorporate estimates of uncertainty in the scale of the modifications as we construct the minimum and maximum models.

4.1. Initial topography

Our starting point for topography is the BEDMAP dataset of Lythe et al. (2001), downsampled to 10-km grid spacing (Fig. 2a). In the Marie Byrd Land area of West Antarctica, several recent studies have reported significant improvements to the topographic database (Luyendyk et al., 2003; Behrendt et al., 2004; Holt et al., 2006; Vaughan et al., 2006; Wilson and Luyendyk, 2006), and we incorporate these updates in our grid (Fig. S1). Additionally, we remove several volcanic edifices younger than 34 Ma in Marie Byrd Land and Victoria Land (e.g. LeMasurier and Rex, 1989). For simplicity, and because the edifices may be associated with significant intrusive bodies, we do not account for isostatic compensation of the edifices.

4.2. Ice load

Our restoration for load of the modern ice closely follows Wilson and Luyendyk (2009). We start with a small restoration for the ongoing rebound for ice removed since the Last Glacial Maximum. This effect is poorly known (e.g. James and Ivins, 1998) so we use the model for present vertical motion of Denton et al. (1991) multiplied by 3000 years. The maximum change is a ca. 50 m increase in the elevation of the southern Antarctic Peninsula. Next we apply the weight of the current grounded ice from BEDMAP as an upward load and calculate flexural rebound as previously described. The resulting topography is shown in Fig. 2b.

4.3. Thermal subsidence

Our restoration for thermal subsidence in the WARS also closely follows Wilson and Luyendyk (2009). The tectonic extension history is approximated as a series of adjacent, non-overlapping regions each

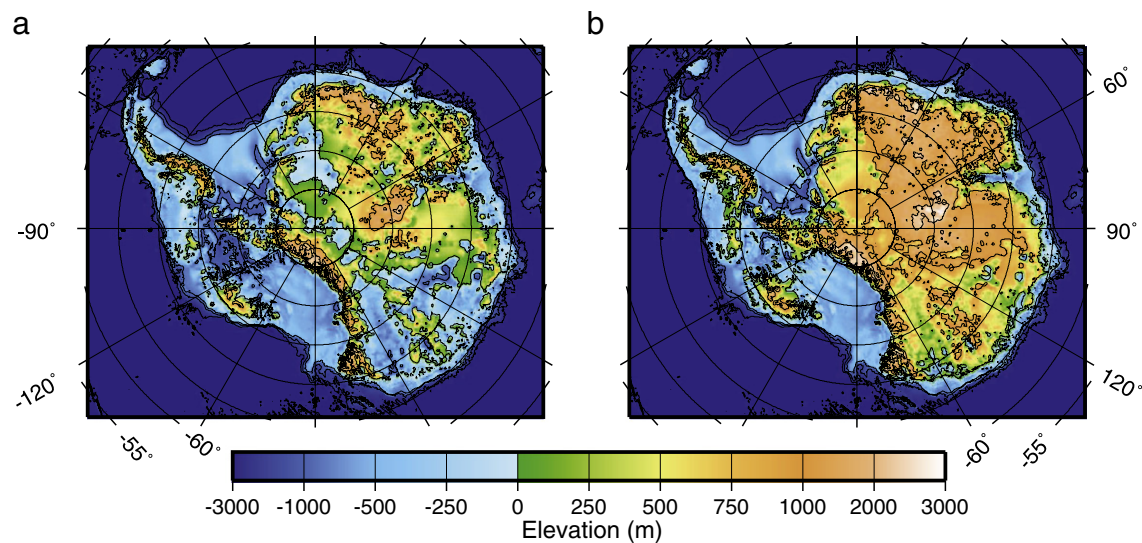


Fig. 2. (a) Present-day Antarctic bed topography, slightly updated from BEDMAP (Lythe et al., 2001). (b) Topography after isostatic rebound from removal of the present-day ice load.

with a uniform stretching factor and an instantaneous extension age. This simplification allows application of McKenzie's (1978) 1-D model for subsidence in response to increase of the thermal gradient during extension. We calculate predicted subsidence within each region in the absence of a water load and smooth the resulting grid on a scale of 40 km to approximate horizontal heat conduction. We then iteratively calculate the flexural isostatic response to flooding the subsided area with water. For our maximum reconstruction, we use a slight modification of the thermal subsidence model as Wilson and Luyendyk (2009, Fig. S2), but for the minimum reconstruction we reduce the thermal subsidence by a factor of 0.9 and recalculate the isostatic response to flooding as a simple model of potential overestimation of subsidence.

4.4. Shelf sedimentation

In the Ross Sea, we remove stratigraphic units RSS-2 and younger, as mapped by ANTOSTRAT (1995). Under the Ross Ice Shelf, our minimum surface uses the same sediment thickness as Wilson and Luyendyk (2009), following the assumption that most of area has incurred net sedimentation. In contrast, our maximum surface follows the assumption that most of the area has incurred net erosion. In the Weddell Sea, we remove sediment to the W4 reflector of Rogenhagen et al. (2004), extrapolated to the western Weddell Sea (Fig. S3). We apply flexural compensation of the sediment load based on a density of 2300 kg/m³.

4.5. Horizontal plate motion

The amount of relative motion between East and West Antarctica since 34 Ma in the Ross Sea is well constrained at about 70 km by the anomaly C13 reconstruction of Cande et al. (2000). We use the same finite rotation as Wilson and Luyendyk (2009) (71.5°S, 35.8°W, 1.14°) to extrapolate this motion across the WARS. This alternative, within the Cande et al. (2000) confidence interval, tapers the relative motion to about one-third of the Ross Sea value where we connect the plate boundary to the triple junction with the Phoenix plate at the subduction zone adjacent to the Antarctic Peninsula. We include small motion to undo back-arc spreading at Bransfield Strait (68.5°S, 79°W, −3.2°). We also include motion of the South Orkney microplate (68.2°S, 34.4°W, 12.60°) following Eagles and Livermore (2002). Because the motions since 34 Ma are relatively small, we simply

remove grid cells in the extended area and translate West Antarctic elevations based on the finite rotations (Fig. S4).

4.6. East Antarctic erosion restoration

We underpin our erosion restoration model with a set of assumptions. The beds of former northern hemisphere ice sheets show that an array of glacial features would be expected to evolve as an ice sheet waxes and wanes (Kleman et al., 2008). These range from small-scale alpine glacial features on localised highlands, to large-scale radial troughs incised at the coast under continental-scale ice conditions. Glacial erosion has lowered the interior of Scandinavia by on the order of 10's of meters during the Quaternary. We assume that similar landscapes evolved at comparable rates in Antarctica where ice sheets have fluctuated between local, regional and continental scales since 34 Ma. We also assume that the large-scale coastal troughs that drain East Antarctica already existed at the E–O boundary and have since been enhanced by selective glacial erosion (Jamieson and Sugden, 2008; Jamieson et al., 2010). For glacial troughs to evolve and selective erosion to occur, an existing topographic feature must have existed, probably in a lower amplitude form, before the growth of an ice mass. Evidence for the pre-existence of valley systems includes the Palaeozoic–Mesozoic age Penck–Jutul Trough in Dronning Maud Land, and the Mesozoic Lambert graben (Mishra et al., 1999; Näslund, 2001). On shorter timescales, geomorphic evidence indicates that parts of the Transantarctic Mountains retain signals of pre-glacial fluvial incision and passive-margin development (Baroni et al., 2005; Jamieson and Sugden, 2008) and that much of East Antarctica may retain its large-scale fluvial drainage spacing (Jamieson et al., 2005).

We simulate a set of 13 successively larger 'steady-state' ice masses over Antarctica following and extending the approach of Jamieson et al. (2010). Their extents are not prescribed, but instead reflect the simplicity with which the modeled climate is stepped from a 'Patagonian' regime towards a 'Polar' regime in order to generate equilibrium glacial configurations. Given the stepwise history of key climate changes for Antarctica since the Oligocene (Table 2), each of the configurations are assigned to a time period so that we can calculate the overall lifespan of each scale of ice sheet. By calculating erosion potential for each ice mass scenario and scaling it by the length of time over which it may have existed, we calculate total erosion potential. Sensitivity tests reflect the uncertainty in our understanding of ice sheet history between 33.6 and 14 Ma and therefore the potential variation in the scales and erosive capacity of

ice sheets during that time. Additional uncertainty is inherent in the model due to the difficulty of predicting the onset zone for basal melting in the interior of East Antarctica because of potential sensitivity to changes in geothermal heat flux (Pollard et al., 2005; Jamieson et al., 2008). However, because this onset zone tends to be found on flatter areas of the bed where the ice surface gradient is shallow and where streaming does not occur at the present day, modeled sliding velocities are never high. Therefore the error in erosion potential resulting from uncertainties in geothermal heat flux, which is kept constant at 42 mW/m^2 , is likely to be small. The final erosion potential calculation reflects an intermediate-scaled set of modeled ice sheet scenarios (Fig. 3).

To obtain a final maximum and minimum erosion estimate for East Antarctica, erosion potential is adjusted so that: 1) incision does not exceed present day trough depths; 2) incision is limited to zero where cold-based ice is predicted to have protected the landscape; 3) inland erosion is within reasonable bounds as defined by extrapolating Quaternary erosion patterns in the Scandinavian ice sheet (Stroeven et al., 2002; Kleman et al., 2008); 4) total erosion reflects either the maximum or the minimum offshore sediment volumes after adjustment for biogenic fraction and compaction. The latter step requires individual scaling of drainage basin 'erodibility', which was initially assumed to be uniform across the continent, so that the correct sediment volumes are produced by each basin (Table 3). Scaling factors for each basin reflect the upper and lower error bounds for offshore sediment volumes.

Our initial attempts to restore glacial erosion tended to fill the coastal valleys whilst only replacing a fraction of the total source volume deduced from offshore sediment volume. We therefore infer that the model underpredicts the amount of material eroded from zones where ice slides at low-to-medium velocities. Accordingly, we scale the erosion calculation using power-law of less than 1 so that the contribution of intermediate basal ice velocities to erosion rates is enhanced relative to minimum and maximum rates. This adjustment is the equivalent of making an adjustment in the relationship between basal melt-rate and basal slip so that efficient erosion can be achieved with less water at the bed than initially assumed. We find that if the

power is too small, erosion is over-balanced towards the interior of East Antarctica. If it is too large the coastal troughs are overfilled. A continent-wide exponent of 0.4 satisfies constraints provided by offshore sediment volume and coastal trough depth, and compares well with expected rates of erosion inferred from interior zones of ice sheets in the Northern hemisphere (Kleman et al., 2008). The modeled pattern of erosion is shown in Fig. 4.

4.7. West Antarctic erosion restoration

Existing ice sheet and glacial erosion models are not suited to marine-based systems like West Antarctica which are underlain by soft sediment, the deformation of which means that the links between mechanical erosion and ice velocity decouple. Thus, for the large amounts of erosion needed to restore the non-cratonal areas of West Antarctica we employ a constrained system of surface fitting. Following Wilson and Luyendyk (2009), we fit a smooth surface to a series of trial points above the topography, determine the load removed by subtracting the topography from the trial surface (assuming a uniform rock density of 2500 kg/m^3 as a simple average for both sediment and basement), and calculate isostatic compensation of the restored surface. We iteratively adjust the trial surface to fit constraints including the source volume inferred from sediment volume (Table 1) and the assumption that modern glacial drainage approximately follows the pre-34-Ma drainage. We join the separate models for East and West Antarctic erosion by allowing the predictions to overlap and simply taking the maximum.

For the area of the Ronne-Filchner Ice Shelves, draining to the Weddell Sea, our maximum model follows the assumption that the area in the Eocene was a mature sedimentary basin, filled to approximately Eocene sea level. In contrast, our minimum model assumes sediment supply was not adequate to fill the basin. Alternatives for restored regional average elevation ranging from near sea level to near -500 m are permitted by the poorly known offshore sediment volume. For the Ross and Amundsen Sea drainages, relations between sediment volume, source area, and present topography require that most of the drainages reconstruct above sea level. In the latter areas, large differences in erosion thickness produce only moderate changes in predicted topography because isostatic compensation preserves only ca. 20% of the change in thickness as change in surface elevation.

4.8. Special cases

The Lambert graben is an early Mesozoic rift extending well into the continental interior (Mishra et al., 1999). Current water depth does not permit grounding of ice, even for ice sheets moderately thicker than at present (Taylor et al., 2004). Because of the age of the graben, we assume it had filled with sediments to sea level by the Eocene. We use iterative surface fitting as used for most of West Antarctica to model the post-Eocene erosion of the graben fill.

LeMasurier and Landis (1996) argue that the present highlands of Marie Byrd Land have been uplifted from near sea level since Eocene by mantle plume activity. While this suggestion remains controversial, we allow for the possibility by adjusting our minimum model by subtracting an elliptical dome surface, dimensions $1000 \times 500 \text{ km}$, with maximum amplitude of 1 km (Fig. S5). Our maximum model does not include this adjustment.

5. Results and discussion

In general, our model-eroded volumes (Table 3) are within reasonable bounds of the target volumes derived from observed sediment volumes (Table 1). Exceptions include the Dronning Maud Land and Enderby Land sectors ($0\text{--}60^\circ\text{E}$), where we limit the restored eroded volume to avoid overfilling coastal troughs. Our model-eroded

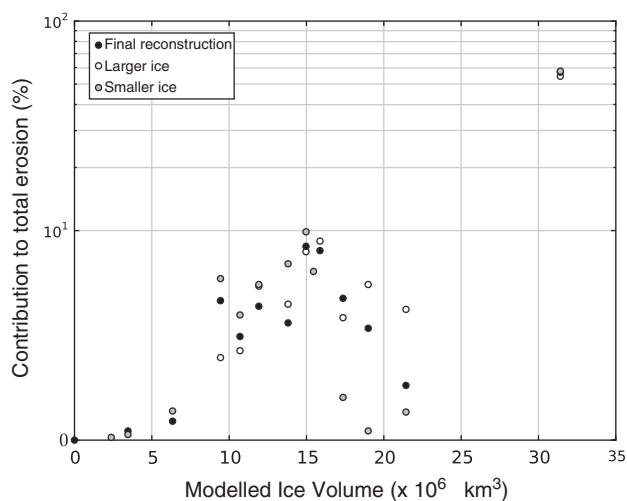


Fig. 3. Ice sheet scales and their contributions to modeled sediment restoration. The most significant contribution of sediment (between 50 and 60%) comes from the continental-scale ice sheet. The distinction between scales of ice sheet follows a similar approach to Jamieson et al. (2010) and reflects the size of steps in climate forcing used to generate successively larger steady-state ice masses. Sensitivity tests using larger or smaller ice sheets in the periods between 33.6 and 14.2 Ma show that variation in ice-sheet scale does not significantly change the overall pattern of eroded sediment. However, in analysing the difference between the small and large ice scenarios, the model is shown to be sensitive to uncertainty in the longevity of ice volumes of over 16 million km^3 volume. Therefore an intermediate longevity for such ice volumes is assumed in the final reconstruction.

Table 3
Modeled eroded volume restored.

Region		Minimum model				Maximum model			
Name	Longitude	Target volume (10 ⁶ km ³)	Model volume (10 ⁶ km ³)	Area 10 ⁶ km ²	Average thickness (km)	Target volume 10 ⁶ km ³	Model volume 10 ⁶ km ³	Area 10 ⁶ km ²	Average thickness (km)
DML	0°–30°E	0.34	0.30	0.57	0.52	0.54	0.30	0.57	0.52
EL	30°–60°E	0.40	0.37	0.69	0.55	0.63	0.37	0.69	0.55
MRL-PEL	60°–94°E	0.75	0.83	1.96	0.42	1.17	1.16	1.96	0.59
QML-WL	94°–124°E	0.34	0.37	1.78	0.21	0.54	0.53	1.78	0.30
G5L-OL	124°–165°E	0.31	0.34	1.34	0.25	0.59	0.51	1.34	0.38
Ross	165°E–150°W	1.03	1.24	2.17	0.57	2.73	2.35	2.34	1.00
Bell-Amun	150°–80°W	1.02	1.13	1.03	1.10	2.21	1.75	1.03	1.70
W Penins	80°–50°W	0.64	0.29	0.50	0.58	1.70	0.38	0.51	0.75
Weddell	~50°W–0°	1.71	2.38	3.81	0.63	4.18	3.70	3.82	0.97
Totals:		6.54	7.25	13.85	0.52	14.29	11.05	14.04	0.79

volumes here, the same for our maximum and minimum models, are slightly below the minimum target values. In western Dronning Maud Land, [Jacobs and Lisker \(1999\)](#) infer that a large volume of Jurassic lava was eroded from the present highlands by 100 Ma. We speculate that at 34 Ma, much of the resulting sediment was on the shallow continental shelf, and was later eroded and redeposited in deep water. We have not attempted to tune the model for such an erosion pattern that departs from predictions based on the assumption of ice acting on a uniform substrate. A more serious mismatch occurs for the Antarctic Peninsula, where fitting the minimum and maximum target volumes would require average eroded thicknesses of 1.3 and 3.4 km, respectively. We probably have underestimated the erosion of the southern Peninsula, the only place with enough room to provide the source volume. For the Ross, Amundsen, and Weddell sectors, where the uncertainty in the volume of observed sediment is large and subjective, and the effort to revise the model erosion volume is significant, we have not forced the model volumes to the full range of the targets estimated from sediment volume. We allow a moderate buffer so that the models are not likely to be rendered obsolete by modest improvements in our knowledge of the offshore sediment volume.

In West Antarctica, our reconstructions ([Fig. 5](#)) contain a substantial upland feature as a result of the infilling of the Ross Sea and Amundsen Sea sectors. The large volumes of sediment offshore of these sectors require a minimum average reconstructed elevation slightly above present sea level and permit an average elevation many

hundreds of meters higher. Our reconstruction is certainly artificially smooth, as horst-and-graben fabric visible in ice-penetrating radar ([Luyendyk et al., 2003; Behrendt et al., 2004](#)) would be expected to have already been present prior to glacial erosion.

In East Antarctica, the changes to the topography are more subtle because the volume of sediment restored is smaller ([Table 3](#)), but the area over which it is distributed is larger. Key features include the partial filling of coastal troughs including the Lambert graben which is filled to near present day sea level ([Taylor et al., 2004](#)) but remains a significant feature ([Mishra et al., 1999](#)). Our erosion model predicts that highland areas now buried under cold-based zones of the East Antarctic ice sheet existed on a similar scale to present in the Oligocene. For example on the Gamburtsev subglacial mountains our topographies retain the alpine glacial landscape which was recently mapped by [Bo et al. \(2009\)](#) thus adding to evidence suggesting it was sculpted before the E–O boundary and continental-scale glaciation. In Dronning Maud Land we change the upland areas very little. This is consistent with evidence that although focussed glacial erosion by wet-based ice and local alpine glaciers in the Jutulssessen area excavated a ca. 1200 m deep valley system at between 34 and 14 Ma, an early Permian palaeo-plateau is otherwise preserved ([Näslund, 1997, 2001](#)).

On the flanks of the Gamburtsev subglacial mountains, the depression which now contains subglacial Lake Vostok is intact but is shallower at the E–O boundary according to our reconstructions. Other subglacial overdeepenings of varying scales including the

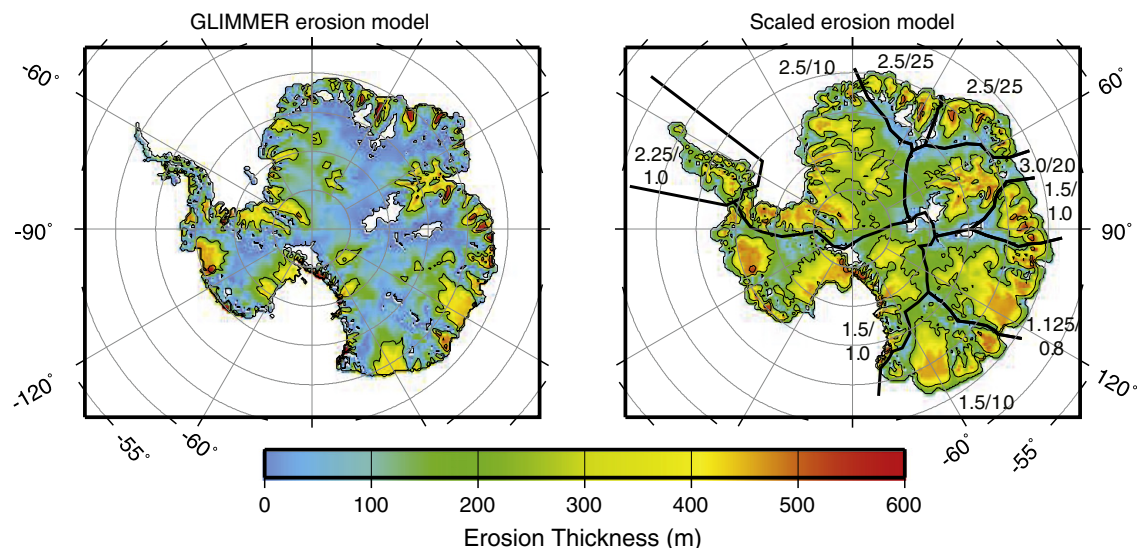


Fig. 4. Modeled erosion pattern before (left) and after (right) power-law scaling. Maximum and minimum scaling factors for each drainage system are noted outboard of each system. The scaling factors tune the erosion volumes to match the targets based on sediment volumes with the caveat that drainage valleys should not be overfilled.

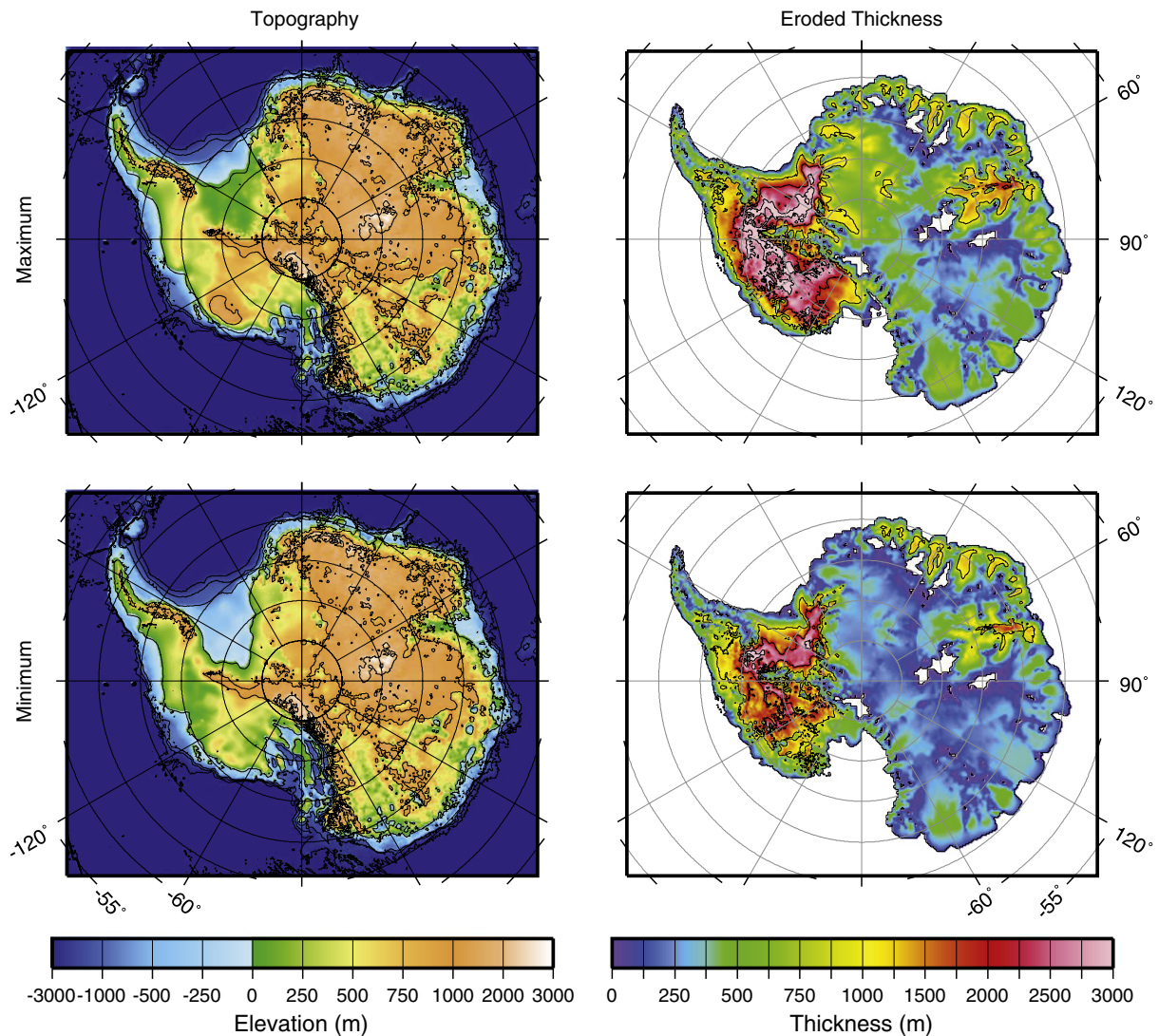


Fig. 5. Maximum and minimum reconstructed topography and eroded thickness maps, 1000-m contour interval. Land area above present sea level is 13.0×10^6 km² for the maximum and 12.4×10^6 km² for the minimum, compared with 10.5×10^6 km² for the ice-rebounded modern topography of Fig. 2b. The maximum and minimum reconstructed topographies are available to download in the supplementary information or via www.antscape.org.

Aurora and Wilkes basins are not significantly different to the present day. Indeed, across much of the interior of East Antarctica, our model suggests that the landscape has been lowered by less than 300 m since the E–O boundary. This is in line with the depths expected if rates from the shorter-lived northern hemisphere glacial landscapes such as Scandinavia are extrapolated over longer periods (Kleman et al., 2008).

Important constraints for several aspects of our reconstruction come from the geologic record at DSDP Site 270 in the Ross Sea, which shows an Oligocene marine transgression over terrestrial regolith (palaeosol) on basement gneiss now at ~1000 m below sea level (Ford and Barrett, 1975; Hayes et al., 1975). DeSantis et al. (1999) tested simple models for sediment loading and thermal subsidence of this area and found few models consistent with this rather large subsidence for an area often considered tectonically stable through the Cenozoic. They found that either the effective elastic lithosphere must be very thick (70 km) for the load of thick sediment in the adjacent basin to drive the subsidence, or the time of tectonic extension must be younger than the commonly assumed 90–100 Ma for thermal contraction to drive the subsidence. Our results are generally similar, with the Site 270 basement most easily restoring above sea level at 34 Ma if extension in the central Ross Sea is younger

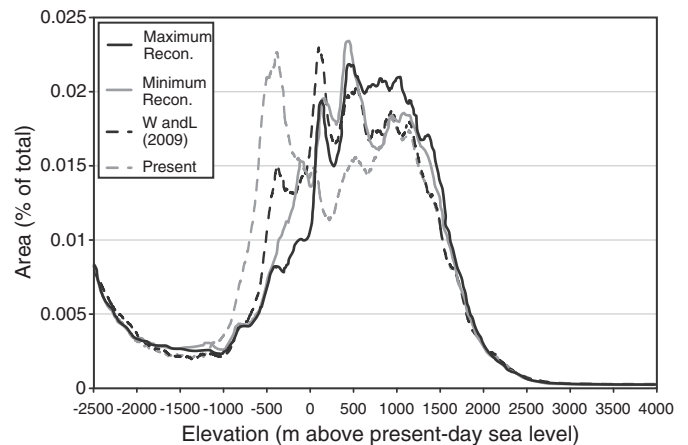


Fig. 6. Hypsometry of Antarctic topographies comparing fraction of land surface area against elevation. This illustrates the shift between land below sea level at present day to land above sea level in the reconstructions. Solid black line: Maximum reconstruction; Solid grey line: Minimum reconstruction; Dashed black line: Reconstruction presented in Wilson and Luyendyk (2009); Dashed grey line: Present day topography rebounded for ice load removal as used as our boundary condition for the reconstructions.

than 70 Ma with a stretching factor at least 2.0. Our maximum model restores the site to 120 m above modern sea level, while our minimum, with slightly reduced thermal subsidence, restores to 30 m. Larger reductions in modeled thermal subsidence would not satisfy the observational constraint here. We found that for models with thin elastic lithosphere (20 km or less), isostatic compensation was essentially local and extreme models of recent extension or high stretching factor would be required for basement to have subsided 1000 m since after 34 Ma. These experiments guided our choice of the simplifying assumption of a uniform elastic thickness of 35 km.

We compare the hypsometry of our reconstructions against a previous reconstruction of West Antarctica (Wilson and Luyendyk, 2009) and the present day bed dataset used as the basemap for our reconstruction (Fig. 6). Hypsometric analysis of the reconstructions elucidates the changes in distribution of land area over elevation. Key differences include a significant increase in area above sea level caused by the filling of the Ross and Weddell Seas and the Lambert Trough and the associated decreases in the area at between 0 and 700 m depth. The filling of the Ross and Weddell Seas are strongest in the Maximum reconstruction and the majority of the material restored is added to a source area below 1000 m elevation. Above this height the present hypsometry is very close to that of Wilson and Luyendyk (2009). Thus at elevations above ca. 1000 m, the difference in topographic distribution between the present bed and the reconstructions are the result of sediment restoration in the central uplands of East Antarctica where relatively small amounts of material are distributed over a wide area.

The implications of the differences in topography between present day and our reconstructions are that the feedbacks between topography and climate would support increased ice volume at the E–O boundary. Much of this would result from the changes in West Antarctica with the increased elevations in East Antarctica making a small but nonetheless important contribution. Compared with an area above modern sea level of $10.5 \times 10^6 \text{ km}^2$ for the ice-rebounded modern topography of Fig. 2b, our minimum reconstruction has an area of $12.4 \times 10^6 \text{ km}^2$ above modern sea level, and our maximum, $13.0 \times 10^6 \text{ km}^2$. We suggest that volume may be on the order of magnitude that is currently lost in the gap between ice volume records and modeled ice sheets (e.g. DeConto et al., 2008; Miller et al., 2008). Any Early Oligocene ice sheet in West Antarctica would not have been marine-based in nature as hitherto assumed in models of E–O ice. Rather, we suggest that Early Oligocene West Antarctic Ice Sheet was dynamically different due to its terrestrial nature as it would have been grounded to a lesser extent below sea level. Therefore it is likely to have been less responsive to changes in sea level and ocean temperature. This indicates that the dynamics of the ice streams which dominate the drainage of the present day West Antarctic system may have changed significantly over time. For example perhaps such fast-flowing regimes underlain by deformable sediment did not exist on such a scale in the early evolution of the ice sheet. The implication is that as the bed was lowered it may have evolved into a more dynamic marine-based ice sheet, with significant volumes of eroded material being deposited offshore in the West Antarctic Rift System.

The work described herein forms part of the wider ANTscape project to reconstruct palaeotopographies at a range of key transitions over the last ~100 Ma. We anticipate that the E–O boundary reconstructions will be refined in response to a number of future dataset releases. These are likely to include an improved present day dataset along the lines of ALBMAP (Le Brocq et al., 2010) that will provide a more accurate present day topography upon which to base our reconstructions. New high-resolution bed data of the present Antarctic bed, including that introduced by Bell et al. (2011) will strengthen our knowledge of subglacial topography and basal processes in East Antarctica. Improvements in the accuracy of offshore sediment data used to constrain our erosion models are anticipated as

a result of the CASP project to develop an age controlled circum-Antarctic dataset of sediment thicknesses. Ongoing work will also help separate the signals of ice sheet and climate fluctuations recorded in deep sea sediment cores. This will enable higher temporal resolution ice sheet and erosion modeling to be carried out and may clarify the importance of various ice sheet scales in contributing sediment to the shelf. Therefore we anticipate a more accurate picture of onshore glacial erosion dynamics will be made possible.

Supplementary materials related to this article can be found online at doi:10.1016/j.palaeo.2011.05.028.

Acknowledgments

We are grateful to the Scientific Committee for Antarctic Research and to the Antarctic Climate Evolution program for funding and to the ANTscape working group (www.antscape.org) for the discussions from which this paper was developed. We thank Graeme Eagles and an anonymous reviewer for their constructive criticism and encouraging comments. Stewart Jamieson was funded by the Natural Environmental Research Council UK. This material is based upon work supported by the National Science Foundation under Cooperative Agreement No. 0342484 through subawards administered and issued by the ANDRILL Science Management Office at the University of Nebraska-Lincoln, as part of the ANDRILL U.S. Science Support Program.

References

- Anderson, J.B., 1999. Antarctic Marine Geology. Cambridge University Press, Cambridge.
- ANTOSTRAT, 1995. Seismic stratigraphic atlas of the Ross Sea. In: Cooper, A.K., Brancolini, G. (Eds.), *Geology and Seismic Stratigraphy of the Antarctic Margin*. American Geophysical Union, Washington D.C.
- Banks, R.J., Parker, R.L., Huestis, S.P., 1977. Isostatic compensation on a continental scale: local versus regional mechanisms. *Geophysical Journal of the Royal Astronomical Society* 51, 431–452.
- Barker, P.F., Kennett, J.P., Party, S.S., 1988. Proceedings of the Ocean Drilling Program, Initial Reports, Weddell Sea, Antarctica, College Station, Texas.
- Baroni, C., Noti, V., Ciccacci, S., Righini, G., Salvatore, M.C., 2005. Fluvial origin of the valley system in northern Victoria Land (Antarctica) from quantitative geomorphic analysis. *Bulletin of the Geological Society of America* 117, 212.
- Barrett, P.J., 1989. Antarctic Cenozoic history from the CIROS-1 drill-hole, McMurdo Sound, Antarctica. *NZDSIR Bulletin* 245 pp.
- Barrett, P.J., 2007. Cenozoic climate and sea level history from glacial marine strata off the Victoria Land coast, Cape Roberts Project, Antarctica. In: Hambrey, M.J., Christoffersen, P., Glasser, N.F., Hubbard, B. (Eds.), *Glacial processes and products: International Association of Sedimentologists Special Publication*, pp. 259–287.
- Bart, P.J., 2001. Did the Antarctic ice sheets expand during the early Pliocene? *Geology* 29, 67–70.
- Behrendt, J.C., LeMasurier, W.E., Cooper, A.K., Tessensohn, F., Trehu, A., Damaske, D., 1991. Geophysical studies of the West Antarctic Rift System. *Tectonics* 10, 1257–1273.
- Behrendt, J.C., Blankenship, D.D., Morse, D.L., Bell, R.E., 2004. Shallow-source aeromagnetic anomalies observed over the West Antarctic Ice Sheet compared with coincident bed topography from radar ice sounding—new evidence for glacial “removal” of subglacially erupted late Cenozoic rift-related volcanic edifices. *Global and Planetary Change* 42 (1–4), 177–193.
- Bell, R.E., Ferraccioli, F., Creyts, T.T., Braaten, D., Corr, H., Das, I., Damaske, D., Frearson, N., Jordan, T., Rose, K., Studinger, M., Wolovick, M., 2011. Widespread persistent thickening of the East Antarctic Ice Sheet by freezing from the base. *Science* 331 (6024), 1592–1595.
- Bertler, N.A.N., Barrett, P.J., 2010. Vanishing polar ice sheets. In: Dodson, J. (Ed.), *Changing climates, earth systems and society*. International Year of Planet Earth. Springer, N.Y., pp. 49–82. doi:10.1007/978-90-481-8716-4_4.
- Bo, S., Siegert, M.J., Mudd, S., Sugden, D., Fujita, S., Xiangbin, C., Yunyun, J., Xueyuan, T., Yuansheng, L., 2009. The Gamburtsev mountains and the origin and early evolution of the Antarctic Ice Sheet. *Nature* 459, 690–693.
- Boulton, G.S., 1972. The role of thermal regime in glacial sedimentation. In: Price, R.J., Sugden, D.E. (Eds.), *Polar geomorphology: Special Publication of the Institute of British Geographers*, 4, pp. 1–19.
- Cande, S.C., Stock, J.M., Müller, D., Ishihara, T., 2000. Cenozoic motion between East and West Antarctica. *Nature* 404, 145–150.
- Cape Roberts Science Team, 1999. Studies from the Cape Roberts Project, Ross Sea, Antarctica. Initial report on CRP-2/2A. *Terra Antarctica* 6, 1–173.
- Cape Roberts Science Team, 2000. Studies from the Cape Roberts Project, Ross Sea, Antarctica. Initial report on CRP-3. *Terra Antarctica* 7, 1–209.
- Cooper, A.K., Brancolini, G., Escutia, C., Kristoffersen, Y., Larter, R., Leitchenkov, G., O'Brien, P., Jokait, W., 2009. Cenozoic climate history from seismic reflection and

- drilling studies on the Antarctic continental margin. In: Florindo, F., Siebert, M. (Eds.), *Antarctic Climate Evolution*. Elsevier.
- DeConto, R.M., Pollard, D., 2003. Rapid Cenozoic glaciation of Antarctica induced by declining atmospheric CO₂. *Nature* 421, 245–249.
- DeConto, R.M., Pollard, D., Harwood, D., 2007. Sea ice feedback and Cenozoic evolution of Antarctic climate and ice sheets. *Paleoceanography* 22, PA3214. doi:10.1029/2006PA001350.
- DeConto, R.M., Pollard, D., Wilson, P.A., Palike, H., Lear, C.H., Pagani, M., 2008. Thresholds for Cenozoic bipolar glaciation. *Nature* 455, 652–656.
- Denton, G.H., Hughes, T.J., 1986. Global ice-sheet system interlocked by sea-level. *Quaternary Research* 26, 3–26.
- Denton, G.H., Prentice, M.L., Burckle, L.H., 1991. Cainozoic history of the Antarctic Ice Sheet. In: Tingey, R.J. (Ed.), *The Geology of Antarctica*. Clarendon Press, Oxford, pp. 365–433.
- Denton, G.H., Wilch, T.I., Sugden, D.E., Marchant, D.R., Hall, B.L., 1993. East Antarctic ice sheet sensitivity to Pliocene climatic change from a dry valleys perspective. *Geografiska Annaler Series A* 75, A (4), 155–204.
- DeSantis, L., Prato, S., Brancolini, G., Lovo, M., Torelli, L., 1999. The Eastern Ross Sea continental shelf during the Cenozoic: implications for West Antarctic ice sheet development. *Global and Planetary Change* 23, 173–196.
- Eagles, G., Livermore, R.A., 2002. Opening history of Powell Basin, Antarctic Peninsula. *Marine Geology* 185, 195–202.
- Fielding, C.R., Naish, T.R., Woolfe, K.J., Lavelle, M.A., 2000. Facies analysis and sequence stratigraphy of CRP-2/2A, Victoria Land Basin, Antarctica. *Terra Antarctica* 7, 323–338.
- Fitzgerald, P.G., Baldwin, S.L., 1997. Detachment fault model for the evolution of the Ross Embayment. In: Ricci, C.A. (Ed.), *The Antarctic Region: Geological Evolution and Processes*. Terra Antarctica Publication, Siena, pp. 555–564.
- Ford, A.B., Barrett, P.J., 1975. Basement rocks of the South-Central Ross Sea, Site 270, DSDP Leg 28. Initial Reports of the Deep Sea Drilling Project, 28, pp. 861–868.
- Hambrey, M.J., Ehrmann, W.U., Larsen, B., 1991. Cenozoic glacial record of the Prydz Bay Continental Shelf, East Antarctica. *Proceedings of the Ocean Drilling Program Scientific Results*. Texas A&M, College Station, pp. 77–132.
- Hayes, D.E., Frakes, L.A., Shipboard Scientific Party, 1975. Sites 270,271,272. In: Hayes, D.E., Frakes, L.A. (Eds.), *Initial Reports of the Deep Sea Drilling Project*, pp. 211–334.
- Holbourn, A., Kuhnt, W., Schulz, M., Erlenkeuser, H., 2005. Impacts of orbital forcing and atmospheric carbon dioxide on Miocene ice-sheet expansion. *Nature* 438, 483–487.
- Hollister, C.D., Craddock, C., 1976. Introduction, principal results—Leg 35 Deep Sea Drilling Project. In: Hollister, C.D., Craddock, C. (Eds.), *Initial Reports of the Deep Sea Drilling Project*, 35, pp. 5–14. U.S. Government Printing Office, Washington D.C.
- Holt, J.W., Blankenship, D.D., Morse, D.L., Young, D.A., Peters, M.E., Kempf, S.D., Richter, T.G., Vaughan, D.G., Corr, H.F.J., 2006. New boundary conditions for the West Antarctic Ice Sheet: subglacial topography of the Thwaites and Smith glacier catchments. *Geophysical Research Letters* 33, L09502.
- Hübscher, C., Jokat, W., Miller, H., 1996. Structure and origin of southern Weddell Sea crust: results and implications. In: Storey, B.C., King, E.C., Livermore, R.A. (Eds.), *Weddell Sea Tectonics and Gondwana Break-up: Geological Society Special Publication*, pp. 201–211.
- Hutter, K., 1983. *Theoretical Glaciology. Mathematical Approaches to Geophysics*. D. Reidel Publishing Company, Boston, Lancaster.
- Jacobs, J., Lisker, F., 1999. Post-Permian tectono-thermal evolution of western Dronning Maud Land, East Antarctica: an apatite fission-track approach. *Antarctic Science* 11, 451–460.
- James, T.S., Ivins, E.R., 1998. Predictions of Antarctic crustal motions driven by present-day ice sheet evolution and by isostatic memory of the Last Glacial Maximum. *Journal of Geophysical Research B: Solid Earth and Planets* 103, 4933–5017.
- Jamieson, S.S.R., Sugden, D.E., 2008. Landscape evolution of Antarctica. In: Cooper, A.K., Barrett, P.J., Stagg, H., Storey, B., Stump, E., Wise, W., 10th ISAES editorial team (Eds.), *Antarctica: a keystone in a changing world*. : Proceedings of the 10th International Symposium on Antarctic Earth Sciences. The National Academies Press, Washington D.C., pp. 39–54.
- Jamieson, S.S.R., Hulton, N.R.J., Sugden, D.E., Payne, A.J., Taylor, J., 2005. Cenozoic landscape evolution of the Lambert basin, East Antarctica: the relative role of rivers and ice sheets. *Global and Planetary Change* 45, 35–49.
- Jamieson, S.S.R., Hulton, N.R.J., Hagdorn, M., 2008. Modelling landscape evolution under ice sheets. *Geomorphology* 97, 91–108.
- Jamieson, S.S.R., Sugden, D.E., Hulton, N.R.J., 2010. The evolution of the subglacial landscape of Antarctica. *Earth and Planetary Science Letters* 293, 1–27.
- Kleman, J., Stroeven, A.P., Lundqvist, J., 2008. Patterns of Quaternary ice sheet erosion and deposition in Fennoscandia and a theoretical framework for explanation. *Geomorphology* 97, 73–90.
- Kuvaas, B., Kristoffersen, Y., Guseva, J., Leitchenkov, G., Gandjukhin, V., Kudryavtsev, G., 2004. Input of glaciomarine sediments along the East Antarctic continental margin: depositional processes on the Cosmonaut Sea continental slope and rise and a regional acoustic stratigraphic correlation from 40 W to 80E. *Marine Geophysical Researches* 25, 247–263.
- Larter, R.D., Barker, P., 1991. Effects of ridge crest–trench interaction on Antarctic-Phoenix spreading: forces on a young subducting plate. *Journal of Geophysical Research* 96, 19,583–19,607.
- Larter, R.D., Cunningham, A.P., Barker, P.F., Gohl, K., Nitsche, F.O., 2002. Tectonic evolution of the Pacific margin of Antarctica 1. Late Cretaceous tectonic reconstructions. *Journal of Geophysical Research* 107, 2345.
- Lawver, L.A., Gahagan, L.M., 1994. Constraints on timing of extension in the Ross Sea region. *Terra Antarctica* 1, 545–552.
- Le Brocq, A.M., Payne, A.J., Veli, A., 2010. An improved Antarctic dataset for high resolution numerical ice sheet models (ALBMAP v1). *Earth System Science Data* 2, 247–260.
- Leitchenkov, G.L., Guseva, Y.B., Gandjukhin, V.V., 2007. Cenozoic environmental changes along the East Antarctic continental margin inferred from regional seismic stratigraphy. In: Cooper, A.K., Raymond, C.R. (Eds.), *Antarctica: A Keystone in a Changing World*. USGS.
- Leitchenkov, G., Guseva, J., Gandjukhin, V., Grikurov, G., Kristoffersen, Y., Sand, M., Golynsky, A., Aleshkova, N., 2008. Crustal structure and tectonic provinces of the Riiser-Larsen Sea area (East Antarctica): results of geophysical studies. *Marine Geophysical Researches* 29, 135–158.
- LeMasurier, W.E., Landis, C.A., 1996. Mantle plume activity recorded by low relief erosion surfaces in West Antarctica and New Zealand. *Geological Society of America Bulletin* 108, 1450–1466.
- LeMasurier, W.E., Rex, D.C., 1989. Evolution of linear volcanic ranges in Marie Byrd Land, West Antarctica. *Journal of Geophysical Research* 94, 7223–7236.
- Lewis, A.R., Marchant, D.R., Ashworth, A.C., Hemming, S.R., Machlus, M.L., 2007. Major middle Miocene global climate change: evidence from East Antarctica and the Transantarctic Mountains. *Geological Society of America Bulletin* 119, 1449–1461.
- Luyendyk, B.P., Wilson, D.S., Siddoway, C.S., 2003. Eastern Margin of the Ross Sea Rift in western Marie Byrd Land, Antarctica: crustal structure and tectonic development. *Geochimistry Geophysics Geosystems* 4, 1090.
- Lythe, M.B., Vaughan, D.G., the BEDMAP Consortium, 2001. BEDMAP: a new ice thickness and subglacial topographic model of Antarctica. *Journal of Geophysical Research* 106 (B6), 11335–11351.
- Mackintosh, A., White, D., Fink, D., Gore, D.B., Pickard, J., Fanning, P.C., 2007. Exposure ages from mountain dipsticks in Mac. Robertson Land, East Antarctica, indicate little change in ice-sheet thickness since the Last Glacial Maximum. *Geology* 35, 551–554.
- Mackintosh, A., Gollidge, N., Domack, E., Dunbar, K., Leventer, A., White, D., Pollard, D., DeConto, R., Fink, D., Zwart, D., Gore, D., Lavoie, C., 2011. Retreat of the East Antarctic ice sheet during the last glacial termination. *Nature Geoscience* 4, 195–202.
- McDougall, I., 1977. Potassium–argon dating of glauconite from a greensand drilled at Site 270 in the Ross Sea, DSDP Leg 28. In: Hayes, D.E., Frakes, L.A. (Eds.), *Initial Reports of the Deep Sea Drilling Project*, Washington D.C., pp. 1071–1072.
- McKenzie, D., 1978. Some remarks on the development of sedimentary basins. *Earth and Planetary Science Letters* 40, 25–32.
- Mildenhall, D.C., 1989. Terrestrial palynology. In: Barrett, P.J. (Ed.), *Antarctic Cenozoic history from the CIROS-1 Drillhole, McMurdo Sound: DSIR Bulletin*, 245, pp. 119–127.
- Miller, H., Henriot, J.P., Kaul, N., Moons, A., 1990. A fine-scale stratigraphy of the eastern margin of the Weddell Sea. In: Bleil, U., Thiede, J. (Eds.), *Geological History of the Polar Oceans: Arctic Versus Antarctic*. Kluwer Academic Publishers, pp. 131–161.
- Miller, K.G., Wright, J.D., Katz, M.E., Browning, J.V., Cramer, B.S., Wade, B.S., Mizintseva, S.F., 2008. A view of Antarctic ice-sheet evolution from sea-level and deep-sea isotope changes during the Late Cretaceous–Cenozoic. In: Cooper, A.K., et al. (Eds.), *Antarctica: A Keystone in a Changing World: Proceedings of the 10th International Symposium on Antarctic Earth Sciences*, pp. 55–70.
- Miller, S.R., Fitzgerald, P.G., Baldwin, S.L., 2010. Cenozoic range-front faulting and development of the Transantarctic Mountains near Cape Surprise, Antarctica: thermochronologic and geomorphologic constraints. *Tectonics* 29, TC1003.
- Mishra, D.C., Sekhar, D.V.C., Raju, D.C.V., Kumar, V.V., 1999. Crustal structure based on gravity–magnetic modelling constrained from seismic studies under Lambert Rift, Antarctica and Godavari and Mahanadi rifts, India and their interrelationship. *Earth and Planetary Science Letters* 172, 287–300.
- Naish, T.R., Woolfe, K.J., Barrett, P.J., Wilson, G.S., Atkins, C., Bohaty, S.M., Buckler, C.J., Claps, M., Davey, F.J., Dunbar, G.B., Dunn, A.G., Fielding, C.R., Florindo, F., Hannah, M.J., Harwood, D.M., Henrys, S.A., Krisek, L.A., Lavelle, M., van der Meer, J., McIntosh, W.C., Niessen, F., Passchier, S., Powell, R.D., Roberts, A.P., Sagnotti, L., Scherer, R.P., Strong, C.P., Talarico, F., Verosub, K.L., Villa, G., Watkins, D.K., Webb, P.N., Wonik, T., 2001. Orbitally induced oscillations in the East Antarctic ice sheet at the Oligocene/Miocene boundary. *Nature* 413, 719–723.
- Naish, T., Powell, R., Levy, R., Wilson, G., et al., 2009. Oblivious-paced Pliocene West Antarctic ice sheet oscillations. *Nature* 458, 322–328.
- Näslund, J.O., 1997. Subglacial preservation of valley morphology at Amundsenisen, Western Dronning Maud Land, Antarctica. *Earth Surface Processes & Landforms* 22, 441–455.
- Näslund, J.O., 2001. Landscape development in western and central Dronning Maud Land, East Antarctica. *Antarctic Science* 13, 302–311.
- Näslund, J.O., Jansson, P., Fastook, J., Johnson, J., Andersson, L., 2005. Detailed spatially distributed geothermal heat-flow data for modeling of basal temperatures and meltwater production beneath the Fennoscandian ice sheet. *Annals of Glaciology* 40, 95–101.
- Nitsche, F.O., Gohl, K., Vanneste, K., Miller, H., 1997. Seismic expression of glacially deposited sequences in the Bellinghousen and Amundsen Seas, West Antarctica. In: Barker, P.F., Cooper, A.K. (Eds.), *Geology and Seismic Stratigraphy of the Antarctic Margin 2: American Geophysical Union, Antarctic Research Series*, 71, pp. 95–108.
- Nitsche, F.O., Cunningham, A.P., Larter, R.D., Gohl, K., 2000. Geometry and development of glacial continental margin depositional systems in the Bellinghousen Sea. *Marine Geology* 162, 277–302.
- Pekar, S.F., DeConto, R.M., 2006. High-resolution ice-volume estimates for the early Miocene: evidence for a dynamic ice sheet in Antarctica. *Palaeogeography Palaeoclimatology Palaeoecology* 231, 101–109.
- Pollard, D., DeConto, R.M., 2009. Modeling West Antarctic ice sheet growth and collapse through the last 5 million years. *Nature* 458, 329–332.
- Pollard, D., DeConto, R.M., Nyblade, A.A., 2005. Sensitivity of Cenozoic Antarctic ice sheet variations to geothermal heat flux. *Global and Planetary Change* 49, 63–74.
- Raine, J.L., Askin, R.A., 2001. Terrestrial palynology of Cape Roberts drillhole CRP-3, Victoria Land Basin, Antarctica. *Terra Antarctica* 8.

- Rocchi, S., LeMasurier, W.E., Vincenzo, G., 2006. Oligocene to Holocene erosion and glacial history in Marie Byrd Land, West Antarctica, inferred from exhumation of the Dorrel Rock intrusive complex and volcano morphologies. *Geological Society of America Bulletin* 118, 991–1005.
- Rogenhagen, J., Jokat, W., 2000. The sedimentary structure in the western Weddell Sea. *Marine Geology* 168, 45–60.
- Rogenhagen, J., Jokat, W., Hinz, K., Kristoffersen, Y., 2004. Improved seismic stratigraphy of the Mesozoic Weddell Sea. *Marine Geophysical Researches* 25, 265–282.
- Roy, M., van de Fliedert, T., Hemming, S.R., Goldstein, S.L., 2007. $^{40}\text{Ar}/^{39}\text{Ar}$ ages of hornblende grains and bulk Sm/Nd isotopes of circum-Antarctic glacio-marine sediments: implications for sediment provenance in the southern ocean. *Chemical Geology* 244 (3–4), 507–519.
- Rutt, I.C., Hagdorn, M., Hulton, N.R.J., Payne, A.J., 2009. The 'GLIMMER' community ice sheet model. *Journal of Geophysical Research* 114, F02004.
- Scherer, R.P., Aldahan, A., Tulaczyk, S., Possnert, G., Engelhardt, H., Kamb, B., 1998. Pleistocene collapse of the West Antarctic Ice Sheet. *Science* 281, 82–85.
- Scheuer, C., Gohl, K., Eagles, G., 2006a. Gridded isopach maps from the South Pacific and their use in interpreting the sedimentation history of the West Antarctic continental margin. *Geochemistry, Geophysics, Geosystems* 7, Q11015.
- Scheuer, C., Gohl, K., Larter, R.D., Rebesco, M., Udintsev, G., 2006b. Variability in Cenozoic sedimentation along the continental rise of the Bellingshausen Sea, West Antarctica. *Marine Geology* 277, 279–298.
- Shevenell, A.E., Kennett, J.P., Lea, D.W., 2004. Middle Miocene Southern Ocean cooling and Antarctic cryosphere expansion. *Science* 305, 1766–1770.
- Siddoway, C.S., Baldwin, S.L., Fitzgerald, P.G., Fanning, C.M., Luyendyk, B.P., 2004. Ross Sea mylonites and the timing of continental extension between East and West Antarctica. *Geology* 32, 57–60.
- Stroeve, A.P., Fabel, D., Harbor, J., Hattestrand, C., Kleman, J., 2002. Quantifying the erosional impact of the Fennoscandian ice sheet in the Tornetrask–Narvik corridor, northern Sweden, based on cosmogenic radionuclide data. *Geografiska Annaler* 84A (3–4), 275–287.
- Sugden, D., Denton, G., 2004. Cenozoic landscape evolution of the Convoy Range to Mackay Glacier area, Transantarctic Mountains: onshore to offshore synthesis. *Bulletin of the Geological Society of America* 116, 840–857.
- Taylor, J., O'Brien, P.E., Cooper, A.K., Leitchenkov, G., Siegert, M.J., Payne, A.J., Hambrey, M.J., 2004. Topographic controls on post-Oligocene changes in ice-sheet dynamics, Prydz Bay region, East Antarctica. *Geology* 32, 197–200.
- Tucholke, B.E., Houtz, R.E., 1976. Sedimentary framework of the Bellingshausen basin from seismic profiler data. In: Hollister, C.D., Craddock, C. (Eds.), *Initial Reports of the Deep Sea Drilling Project*, 35, pp. 197–227. U.S. Government Printing Office, Washington D.C.
- Vaughan, D.G., Corr, H.F.J., Ferraccioli, F., Frearson, N., O'Hare, A., Mach, D., Holt, J.W., Blankenship, D.D., Morse, D.L., Young, D.A., 2006. New boundary conditions for the West Antarctic ice sheet: subglacial topography beneath Pine Island Glacier. *Geophysical Research Letters* 33, L09501.
- Wilson, D.S., Luyendyk, B.P., 2006. Bedrock platforms within the Ross Embayment, West Antarctica: hypotheses for ice sheet history, wave erosion, Cenozoic extension, and thermal subsidence. *Geochemistry, Geophysics, Geosystems* 7, Q12011.
- Wilson, D.S., Luyendyk, B.P., 2009. West Antarctic paleotopography estimated at the Eocene–Oligocene climate transition. *Geophysical Research Letters* 36, L16302.
- Zachos, J.C., Kump, L.R., 2005. Carbon cycle feedbacks and the initiation of Antarctic glaciation in the earliest Oligocene. *Global and Planetary Change* 47, 51–66.
- Zachos, J.C., Breza, J.R., Wise, S.W., 1992. Early Oligocene ice sheet expansion on Antarctica—stable isotope and sedimentological evidence from Kerguelen Plateau, Southern Indian Ocean. *Geology* 20 (6), 569–573.